HIPAGS '96
Detroit, MI
August 22-24, 1996

CONF-960817--8

BNL-63623

Composite particle production in relativistic Au+Au Collisions at AGS: First results from the E866 Forward Spectrometer @ 2, 4, and 10.8 A·GeV

Karim Ashktorab
Department of Physics
Brookhaven National Laboratory
Upton, NY 11973, USA

for the E866 Collaboration:

BNL - UCBerkeley - UCRiverside - Columbia - INS(Tokyo) - Johns Hopkins - Kyoto - LLNL- Maryland - MIT - Tokyo - Tsukuba - Yonsei(Seoul)

ABSTRACT

Particle spectra were measured for Au+Au collisions at 2, 4, and 10.8 A·GeV using the E866 spectrometers. Recent results on proton emission and composite particle production from the E866 forward spectrometer data taken in 1994 together with the first results from the 1995/6 AGS running period are presented. Preliminary results indicate a decrease in the coalescence scaling coefficient with increasing projectile energy and centrality.

1. Introduction

The E802 collaboration, E802, E859, and E866 has been involved in the study of heavy ion reactions since their availability at AGS. So far, E866 studies of Au+Au collisions has been at 10.8 A·GeV, focusing on single particle spectra and correlation measurements. The lower energy gold beams that recently became available at AGS provide the opportunity to extend these studies of nuclear matter which could perhaps lead to new and interesting phenomena. The study of composite particle production can be used to probe the later stages of relativistic heavy-ion collisions. Coalescence models could provide information on source sizes at freeze-out and help estimate the yields for more exotic composites such as multistrange hypernuclei and antinuclei. Energy and centrality dependence of deuteron data could provide unexpected effects, suppression of the formation of deuterons may indicate an increase in the freeze-out volume which could be an indication of plasma formation [1].

The presented results are based on the 10.8 A·GeV Au+Au data taken in 1994, and 2 and 4 A·GeV data taken in late 1995 and early 1996 AGS running period. The transverse mass distributions for protons and composite particles of mass A<4 (d, t, ^{3}He) at 10.8 A·GeV

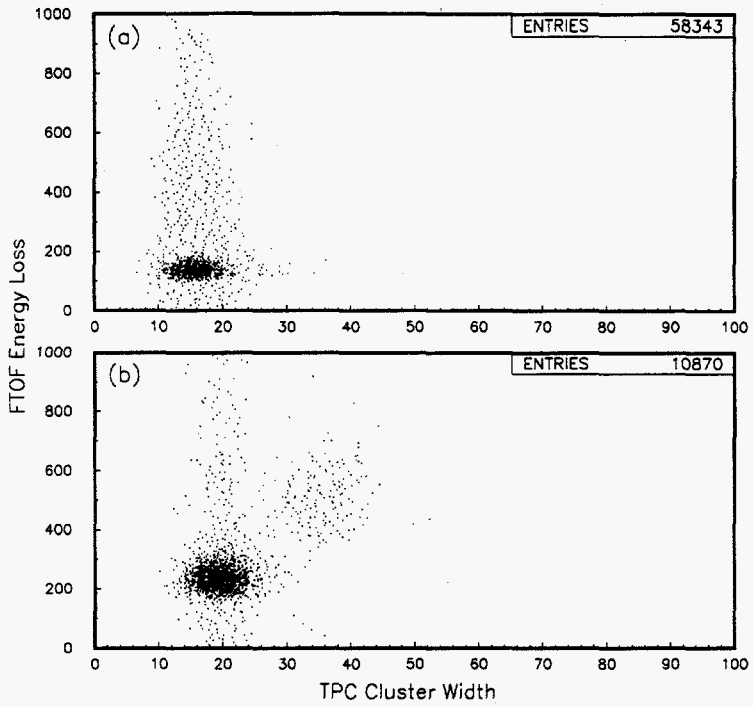

Figure 1: FTOF energy loss (y) vs TPC cluster width (x) for protons (a) and deuterons (b) with momentum 1.5<p<2 GeV/c from Au+Au interactions at 2 A·GeV . The points above y$\tilde{>}$200 in fig. 1a correspond to the Landau tail in the distribution of FTOF energy deposit distribution. The points above x$\tilde{>}$25 and y$\tilde{>}$300 in fig. 1b correspond to α-particles.

are presented together with a brief discussion of the energy and centrality dependence of the coalescence scaling coefficient.

2. Experiment and particle identification

Experiment E866 consists of two magnetic spectrometers, Henry Higgins [2] and the forward spectrometer, together with attendant tracking detectors and time of flight walls, as well as global detectors for event characterization. The two spectrometers are complementary in their coverage. The E866 spectrometers together provide excellent phase space coverage at all energies considered here. The forward spectrometer [3] was introduced in 1993 to permit the identification of heavier charged particles at mid-rapidity which is not possible with Henry Higgins at 10.8 A·GeV for Au+Au interactions due to the high particle densities at smaller angles. The data presented in this contribution were taken with the E866 forward spectrometer only which has a relatively small solid angle of $\approx$ 5 msr but has excellent two track separation even at high track densities in 10.8 A·GeV Au+Au collisions at small angles.

Singly charged particles were identified by applying mass-square versus momentum cuts on identified tracks using the timing information from the segmented forward spectrometer time of flight wall (FTOF, consists of 100 slats) and momentum extracted from time projection (TPC) and drift chambers. ^{3}He could also be identified using similar mass-square

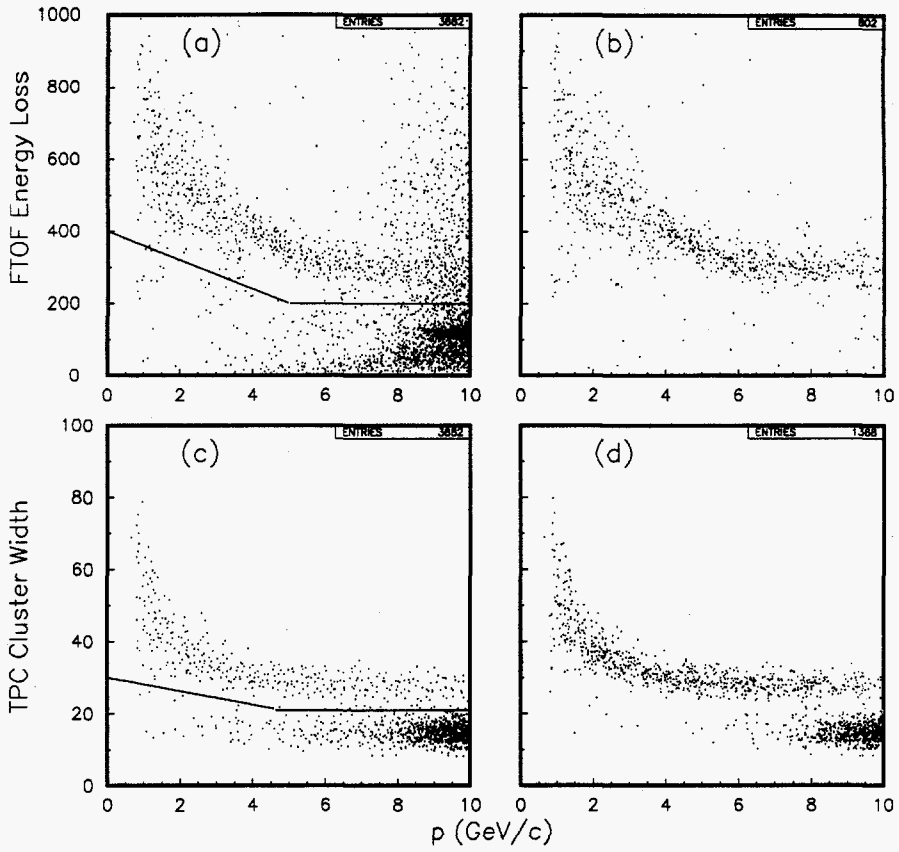

Figure 2: Scatter plots of the energy loss in time of flight slats (FTOF) for tracks satisfying mass-square/momentum cuts for ^{3}He vs. momentum for Au+Au interactions at 10.8 A·GeV with and without TPC cluster width cuts (from fig. 2c) are shown in figures 2b and 2a respectively. The TPC cluster width distribution vs. momentum for tracks satisfying mass-square/momentum cuts for ^{3}He with and without FTOF energy loss cuts (from fig. 2a) are shown in figures 2d and 2c.

vs. momentum cuts. However, due to the scarcity of ^{3}He relative to protons especially at 10.8 A·GeV the "identified" ^{3}He were contaminated by protons. This severely limited the momenta at which ^{3}He could be identified. Since α-particles have almost the same mass/Z ratio as deuterons the above method can not be used to distinguish the α-particles from deuterons. Energy loss information was therefore used to identify helium isotopes. The energy loss from FTOF slats has good resolution and could in principle be used to separate multiply and singly charged particles were it not for the Landau tail in the distribution of the energy deposited in the FTOF slats (The tail is mainly due to the large energy deposited in the FTOF slats by high energy knock-on electrons).

We therefore used the FTOF energy loss together with the TPC cluster widths to separate helium from singly charged particles. The TPCs used in E866 do not have pad readout and were not designed to record dE/dx. They were outfitted with segmented anode wires for better two-particle separation at high particle densities and only the leading and trailing edge times were recorded. The difference in leading and trailing times however gives a crude

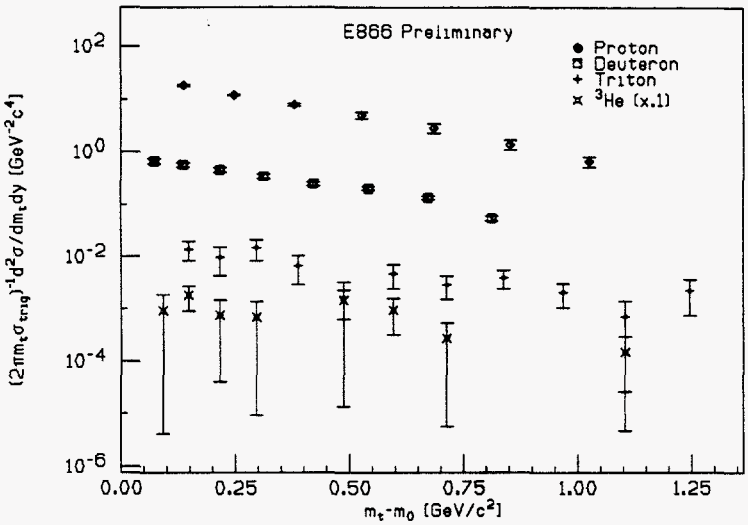

Figure 3: m_t distribution for proton, deuteron, triton, and ^{3}He at 10.8 A·GeV for central (7% of interaction cross section as measured by ZCAL) Au+Au interactions. The spectra correspond to rapidities in the range of 1.4 to 1.6.

measurement of the pulse width. The sum of the difference between trailing and leading edge times for all wires hit corresponding to a track in the TPCs define the TPC cluster width. The TPC cluster width distribution exhibit a reduced Landau tail and a large width relative to that of FTOF distribution, which is due to the larger energy deposited in 1.2 cm of plastic scintillator. Figures 1a and 1b, as an example, show the FTOF energy loss distribution versus TPC cluster width for protons and deuterons of momentum 1.5<p<2 GeV/c in Au+Au collisions at 2 A·GeV. A strong correlation is observed between the energy loss in FTOF and the TPC cluster widths. The α-particles are well separated from the deuterons in Fig. 1b. Fig. 2a show the FTOF energy loss versus momentum for tracks that satisfy mass-square/momentum cuts corresponding to ^{3}He for Au+Au interactions at 10.8 A·GeV. The high momentum contamination in Fig. 2a is mainly due to high energy protons. Fig. 2b shows the same spectrum but with a cut on the TPC cluster width (shown in Fig. 2c) which indicates that the proton contamination is basically removed from the distribution. Figures 2c and 2d show the TPC cluster width distribution for ^{3}He versus momentum without and with FTOF energy loss cut. It is clear that the TPC cluster width provides a more effective tool to separate helium isotopes from singly charged particles. Both FTOF and TPC cluster width cuts were applied to identify ^{3}He in the data presented here.

3. Preliminary Results

Invariant cross sections from the 1994 forward spectrometer data at 10.8 A·GeV are shown in fig. 3 for 1.4<y<1.6. The transverse mass distributions for p, d, t, and ^{3}He shown in the figure correspond to the most central 7% of the interaction trigger ($\approx$ .37 barn) as measured by the zero degree calorimeter, ZCAL. The spectra indicate a decrease in the

logarithmic slope of the spectral shapes of particles with an increase in the particle mass. The spectra were fitted by single exponentials and indicate inverse slopes of 263 ± 10, 395 ± 25, and 445 ± 190 GeV/c^2 for protons, deuterons, and tritons respectively. The decrease in the slope has been attributed to collective transverse nuclear flow [4], an increase in the inverse slopes is predicted as the mass of the emitted particles increase. We will be able to investigate the spectral shapes of the composites more thoroughly from the 1995 high statistics data. It should be noted that efficiency corrections due to multiple scattering have not been included in the present analysis, which could change the spectral shapes of the composites especially at low momenta.

Composite particles emitted near mid-rapidity are expected to be formed at freeze-out at late stages of the evolution of the system resulting from relativistic heavy ion collisions. These particles are likely to be formed by coalescing nuclei once the frequency of interactions has become sufficiently low. In the simple coalescence model a group of nucleons can fuse to produce composite particles if they have a small relative momentum. The probability of the emission of composite particles is given by proton and neutron emission probabilities. The invariant cross section for composite particle production is expressed as the product of the coalescence scaling coefficient and the invariant cross section for the emission of protons raised to the power of the mass number of the composite particle [5,6]:

$$E_A \frac{d^3N_A}{dP_A^3} = B_A (E_p \frac{d^3N_p}{dp_p^3})^A \tag{1}$$

where

$$B_A = A \frac{2s+1}{2^A} (\frac{N_{target} + N_{projectile}}{Z_{target} + Z_{projectile}})^N \frac{1}{N!Z!} (\frac{4\pi}{3m} \tilde{p_0}^3)^{A-1}, \tag{2}$$

N, Z, A, and s are the neutron, proton, mass number, and the spin of the composite particle, E_A, P_A, E_p, and p_p, are the energy and momentum of the composite particle and proton, $P_A = Ap_p$, m is the proton mass, B_A is the coalescence scaling coefficient, and $\tilde{p_0}$ is the coalescence momentum corresponding to the maximum relative momentum of coalescing nuclei which can be expressed in terms of the source size [10]. The above relation indicates that the coalescence scaling coefficient is independent of projectile energy and the centrality of the collision except through $\tilde{p_0}$. Fig. 4 shows the coalescence scaling coefficient for deuteron, triton, and ^{3}He at various energies. The 2, 4, and 10.8 A·GeV data are preliminary results and indicate the values for the coalescence scaling coefficient for peripheral (lowest 50% of the interaction cross section as measured by the E866 zero degree calorimeter, ZCAL) and central collisions (highest 7% of the interaction cross section). The 4 and 10.8 A·GeV data were taken at mid-rapidity and the 2 A·GeV data were measured for rapidities between 1.2 and 1.4. The data at 800 A·MeV correspond to minimum bias Ne+Pb interactions [7]. The 13.7 A·GeV points are from minimum bias and central Si+Pb E814 results [9]. The third point at 10.8 A·GeV was taken from minimum bias Au+Pb interactions reported by E886 [8]. The results indicate a reduction of the coalescence scaling coefficient as the projectile energy increase for all composites, d, t, and ^{3}He. The scaling coefficient is also lower for central interactions. Both effects could be due to the exclusion of the spatial distribution of coalescing nuclei in the model. This could indicate an increase of the source size at freeze-out with energy and centrality. An increase in the source size with centrality has been observed from E866

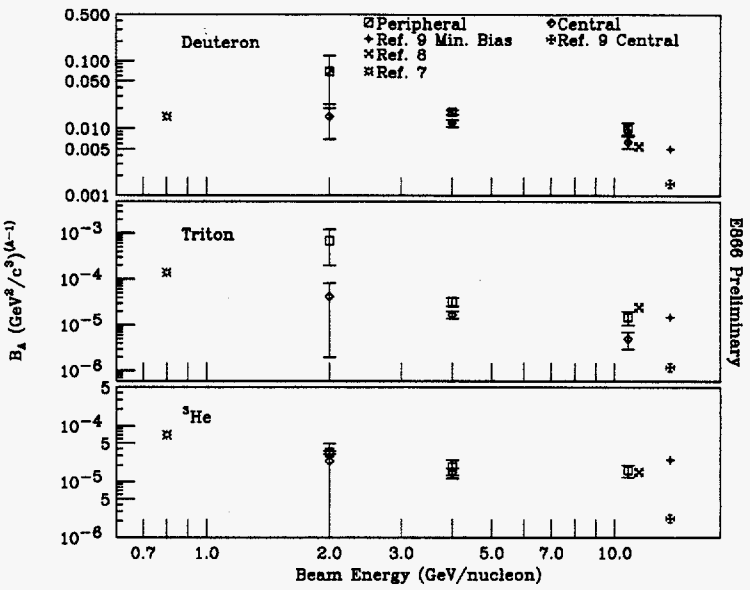

Figure 4: Coalescence scaling coefficient, B_A, versus incident projectile kinetic energy for deuteron (top), triton (middle), and ^{3}He (bottom panel). The point at 800 A·MeV correspond to Ne+Pb minimum bias interactions [7]. The diagonal cross correspond to min. bias Au+Pt results from E886 [8] taken at 10.8 A·GeV. The E886 results were artificially shifted to 11.5 A·GeV in the figure due to its overlap with Au+Au results for clarity. The points at 13.7 A·GeV are E814 min. bias and central Si+Pb data [9]. The symbols (squares and diamonds) at 2, 4, and 10.8 A·GeV are from present work and correspond to peripheral and central Au+Au interactions (No ^{3}He data is shown for Au+Au central collisions at 10.8 A·GeV).

two particle correlation measurement and HBT analysis. More quantitative treatment of coalescence and source sizes will follow upon the availability of final calibrations when the latest data are fully analyzed.

4. Summary

We have measured proton and composite particle yields at 2, 4, and 10.8 A·GeV. An increase in inverse slope parameters with particle mass for p, d, t, ^{3}He could be attributed to nuclear flow. Preliminary results indicate a decrease in the coalescence scaling coefficient with increasing projectile energy and the centrality of the collision. This could be interpreted as an increase in source size at freeze-out. A large number of triggers (over 200 million) was collected at 2, 4, and 10.8 A·GeV during the 1995-96 running period with the two E866 spectrometers that should provide a rich set of physics results in the near future.

5. Acknowledgments

This work was supported by the U.S. Department of Energy under contracts with BNL (DE-AC02-76CH00016), Columbia University (DE-FG02-86-ER40281), LLNL (W-7405-ENG-

48), MIT (DE-AC02-76ER03069), UCRiverside (DE-FG03-86ER40271), by NASA (NGR-05-003-513) under contract with the University of California, by the Ministry of Education, Science and Culture of Japan (under the Japan US agreements on the collaboration in High Energy Physics), and by Ministry of Education and KOSEF in Korea.

6. References

1. D.E. Kahana *et al.*, Phys. Rev. **C54**, 338 (1996).
2. T. Abbott *et al.*, Nucl. Instr. and Meth. **A290**, 41 (1990).
3. K. Shigaki, PhD thesis, Tokyo (1995).
4. R. Mattiello *et al.*, Phys. Rev. Lett. **74**, 2180 (1995).
5. J.L. Nagle *et al.*, Phys. Rev. Lett. **73**, 1219 (1994).
6. L.P. Csernai and J.I. Kapusta, Phys. Rep. **131**, 223 (1986).
7. S. Nagamiya *et al.*, Phys. Rev. **C24**, 971 (1981).
8. N. Saito *et al.*, Phys. Rev. **C49**, 3211 (1994).
9. J. Barrette *et al.*, Phys. Rev. **C50**, 1077 (1994).
10. H. Sato and K. Yazaki, Phys. Lett. **98B**, 153 (1981).